Sizex'92 ERS-1 SAR ice validation experiment

by Stein Sandven, Ola M. Johannessen, Kjell Kloster and Martin Miles

Nansen Environmental and Remote Sensing Center,
Edv. Griegsvei 3a, N-5037 Solheimsvik, Bergen, Norway

ABSTRACT

The Seasonal Ice Zone Experiment (SIZEX 92) project was a sea ice validation experiment for ERS-1 SAR carried out in the Barents Sea in March 1992. ERS-1 SAR images and *in situ* measurements, aerial photographs and video records were obtained from different ice types such as multiyear, firstyear, refrozen leads, pancake ice, grease ice and icebergs. The SAR scenes were downlinked at Tromsø Satellite Station and transmitted to NERSC in near real-time. At NERSC the images were analyzed and sent out to the ships by telefax 2 - 3 hours after the satellite overpass. SAR backscatter values from different ice types were observed and compared with in situ observations during the experiment. Two - three meter thick firstyear ice was the dominant ice type found in a 50 km wide ice edge zone. The SAR backscatter value of this ice ranged from - 10 to -6.5 dB. Firstyear ice further into the ice pack had lower values, from - 13 to - 10 dB. Areas of many multiyear floes were found about 100 km north of the ice edge, at about 78°N. The backscatter value of these floes were typically around -8.5 dB. Refrozen leads with thin ice had low backscatter values, between - 17 and - 13 dB, which were easily distinguishable from the firstyear and multiyear ice. Therefore the ERS-1 SAR seemed to discriminate well between leads, multiyear floes and firstyear ice in the interior of the ice pack. However, in the ice edge zone, where all ice is broken in small floes typically 10 - 100 m large, the SAR was not expected to discriminate between firstyear and multiyear ice. Grease ice had the lowest backscatter of all ice types, ranging from - 20 to - 14 dB, while open water usually had higher backscatter than any of the ice types, from - 4.5 to - 3.0 dB. Thus the ERS-1 SAR seemed to be well capable of detecting the ice edge, at least during winter conditions. In conclusion the ERS-1 SAR scenes studied in the SIZEX 92 experiment provided detailed information on ice edge location, ice concentration, different ice types, ice kinematics, leads/polynyas, shear zones and ice edge processes.

1. INTRODUCTION

The Seasonal Ice Zone EXperiment (SIZEX 92) was the latest in a series of pre- and postlaunch ice validation experiments for ERS-1 SAR (Johannessen et al., 1986). SIZEX 92 was carried out in the Barents Sea in March 1992, using the ice strengthened vessel Polarsyssel and a helicopter (Fig. 1). The research vessel Håkon Mosby operated in open water and in thin ice outside the ice edge. In-situ measurements, aerial photographs and video records were obtained from different ice types in typical winter conditions such as multiyear ice, smooth firstyear ice, young ice types in refrozen leads, broken up firstyear ice, various stages of pancake ice, grease ice and icebergs. In addition open water areas during various wind conditions were documented in order to separate SAR signatures of ice from open water.

Approximately 50 low-resolution SAR scenes (100 m) and 5 full-resolution SAR scenes (25 m) were obtained from ERS-1 during the experiment. The SAR scenes were downlinked at Tromsø Satellite Station and transmitted to NERSC in 2 - 3 hours after observation. AVHRR and SSM/I images were also used in the experiment. All the satellite data were analyzed and sent to the ships by telefax.

2. THE RADAR BACKSCATTER PROBLEM

The radar backscatter from sea ice is highly dependent on physical ice properties such as salinity contents, temperature, surface roughness, snow layers and presence of water. Fig. 2 is a conceptual illustration of active microwave return from multiyear, firstyear (smooth and rough) and open water without wind. Multiyear ice is characterized by low salinity in the surface layer (< 2.0 ‰) which allows penetration of the microwaves into the ice (volume scattering). Firstyear ice, on the other hand, has higher sali-

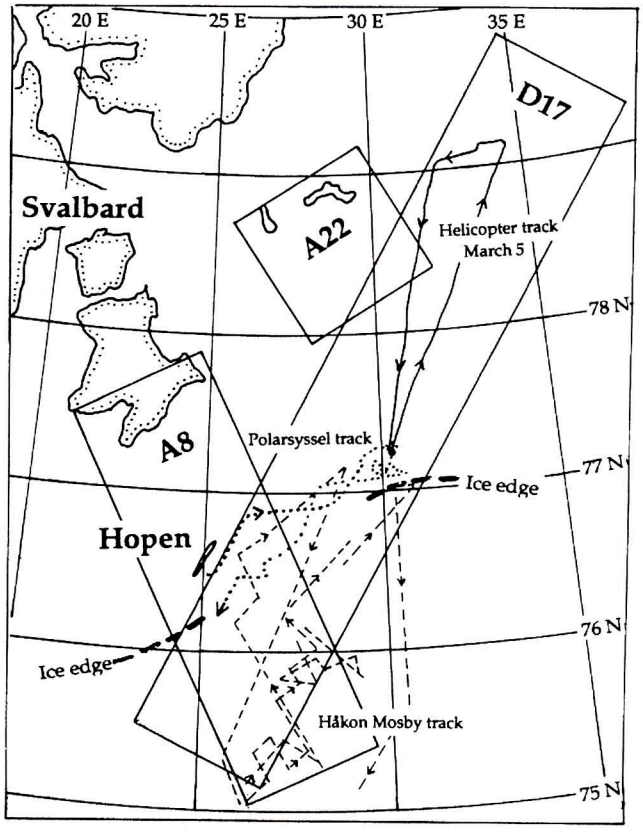

Fig. 1 - Map of the SIZEX 92 experiment area in the Barents Sea. The boxes marked A8, D17 and A22 indicate the SAR coverage from ERS-1 in the experiment area. The dashed line is the track of the R/V Håkon Mosby, the dotted line is the track of R/V Polarsyssel, and the full line is the helicopter track on March 5.

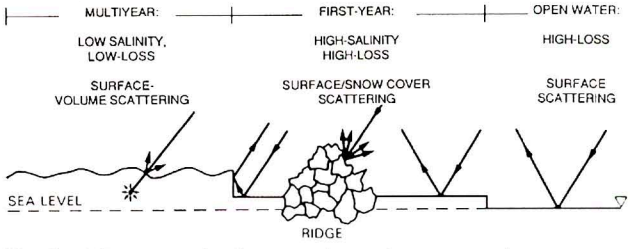

Fig. 2 - Microwave backscatter for multiyear ice, first year ice and smooth open water (Shuchman and Onstott, 1990)

nity in the surface layer (5 - 7 ‰) which causes mainly surface scattering. The volume scattering from the multiyear ice tends to give higher backscatter than the surface scattering from smooth firstyear ice. However, firstyear ice can also give higher backscatter due to rough surface caused by ridges, small floes with many irregular edges and snow crystals. Open ocean gives very low backscatter in the case of no wind, but usually there is some wind which causes short surface waves and high backscatter values (Shuchman and Onstott, 1990). In the SIZEX project some of these problems were addressed in more detail. In particular the capability of the ERS-1 C-band SAR (VV polarization) to classify ice types and separate them from open water signatures in the Barents Sea during winter has been studied (Johannessen et al., 1992).

3. ICE TYPE DETERMINATION

SAR backscatter values from several ice types and open water conditions were analyzed during the experiment. Each image was averaged from 16 x 20 m pixels to 100 m x 100 m pixels, thereby removing much of the speckle noise. The images were then normalized to incidence angle of 23° (in the center of the swath) by applying antenna pattern and incidence angle/distance corrections as described by ESA (Caneva, 1992). Finally, the backscatter values in the images were calibrated to σ_0 values by the relation $\sigma_0 = 20 \log V - 46.9$, where V is the digital value of the 8-bit images analyzed at the Nansen Center. The lowest backscatter observed in the images had values of V = 14 (grease ice) corresponding to the noise floor of - 24 dB. The accuracy of the calibration is about 1 dB.

In situ measurements

The primary in situ measurements were profiles of snow and ice parameters taken at several sites from Polarsyssel and the helicopter. A total of 21 sites were investigated from March 2 to 11. At each site several ice cores were drilled to obtain some spatial statistics of the ice parameters. The ice cores were analysed for temperature, salinity, density and brine volume. Ice type was identified, ice thickness was measured and surface roughness was characterized. Snow thickness, temperature, grain type, grain size, density and layer description were also obtained at each site. An example of a SAR scene extending from open water to the interior of the ice pack is shown in Fig. 3. From the SAR images and the in situ observations the ice conditions in this part of the Barents Sea could be divided into three zones, reflecting different physical processes. In the following discussion each of these zones, which are denoted A, B and C, are described in terms of their SAR signatures.

Zone A. The interior of the ice pack

In the region east of Hopen, many multiyear floes were found about 100 km into the ice pack, north of about 78°N. The backscatter value of these floes were typically -9.0 ±

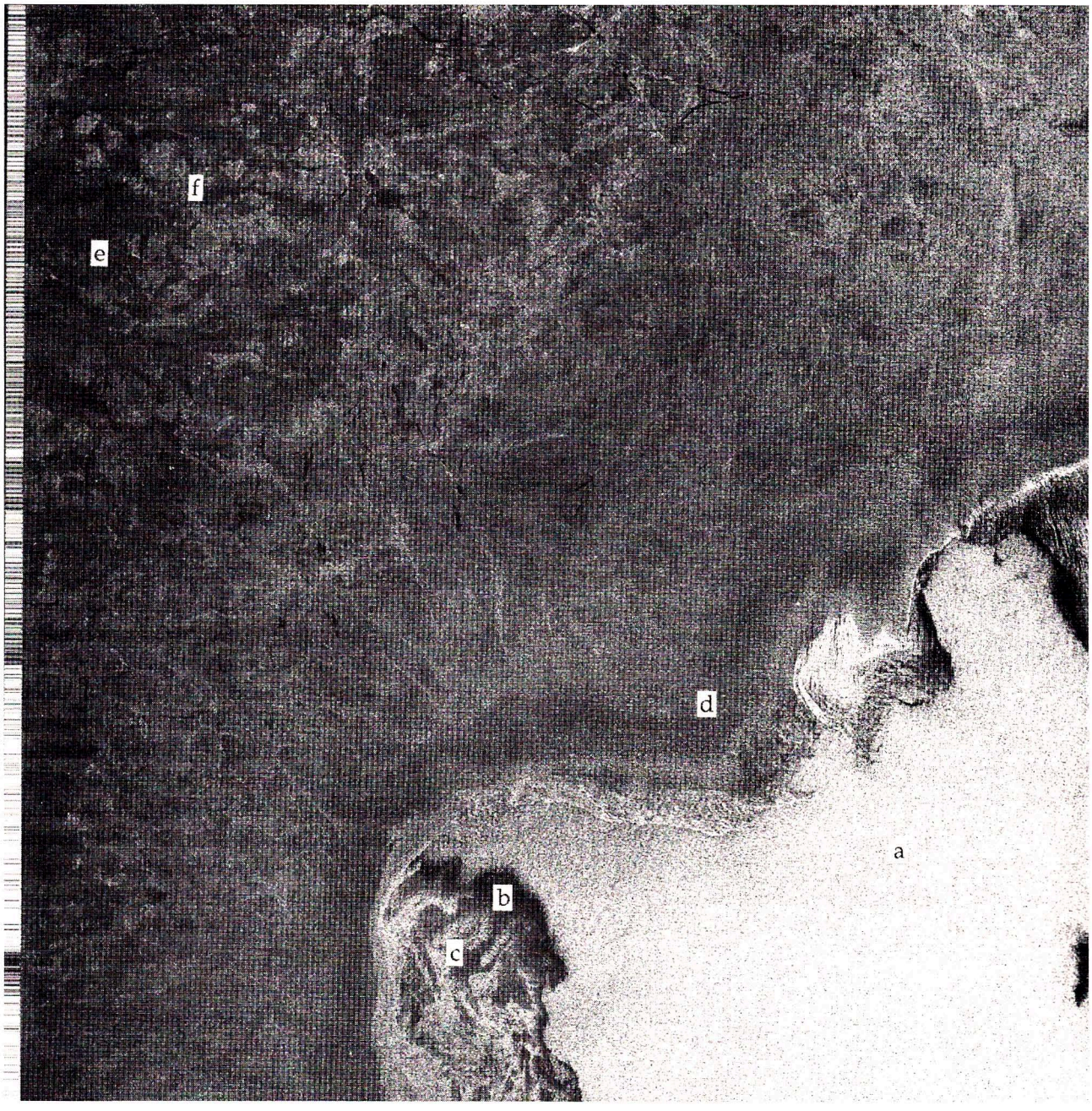

Fig. 3 - ESR-1 SAR image covering 100 x 100 km of the experiment area obtained on March 5. The image shows open water (a), grease ice (b), pancake ice (c), uniform field of 2 - 3 m thick broken-up firstyear ice (d), consolidated firstyear ice in the interior of the ice pack (e), and multiyear floes (f)

1.5 dB. Between the multiyear floes areas of consolidated firstyear ice typically 2 - 3 m thick was observed. This ice had backscatter values from - 10 to - 13 dB. Refrozen leads with smooth thin ice had the lowest backscatter values, between - 19 and - 13 dB. Ridges and leads with open water were found to have variable and higher backscatter, above - 8 dB. In the interior of the ice pack therefore, the ERS-1 SAR demonstrated good capability to discriminate between: a) young ice in refrozen leads, b) multiyear ice in large floes, c) rubble fields/ridges, and d) smooth firstyear ice using simple thresholding of backscatter values.

Zone B. The small floe area.

This zone is characterized by small floes typically 10 - 100 m large, which have been broken up by surface waves penetrating from open ocean into the ice pack. The width of the zone depends on the intensity of the wave field in the preceding days. During the SIZEX experiment the zone was 20 - 30 km wide and was clearly identified in the SAR images as more uniform zone between open ocean and the interior of the ice pack (Fig. 3). The dominant ice type is rough firstyear ice 2 - 3 m thick with backscatter values ranging from -10 to - 6.5 dB. These values are significantly higher than for the consolidated firsyear ice in zone A due to the increased surface roughness. This surface roughness is caused by the edges and ridges of the numerous small floes which cannot be identified in the SAR images. During the experiment the ice concentration was generally high (> 95 %). The open water or thin ice areas between the floes was in the range of 1 - 10 m, which could not be observed in the SAR images. On March 8, when off-ice winds prevailed, the pack opened up near the ice edge and icefree areas of order 1 km could be identified in the SAR images.

Multiyear floes, which drift southwards with the East-Spitzbergen Current, could also occur in this zone. Similar to the firstyear floes the multiyear floes tended to break up due to the wave field. The SAR signature of small multiyear floes was similar to that of surrounding firstyear floes. Drifting icebergs with a horizontal scale of 100 m and a draft of 5 - 8 m were observed frequently in the zone, but their SAR signature even in full resolution images was diffuse. Reliable observations of these icebergs could not be made by the ERS-1 SAR.

Zone C. The area of ice formation

Most of the ice in the Barents Sea is formed locally as the ice edge advances southwards during the freezing season. In the experiment the areas of ice formation were mapped by SAR images and documented by in situ observations. The first stage in ice formation is grease ice which dampens out the short surface waves and causes low radar return signals. This ice had the lowest backscatter of all ice types, ranging from - 24 to - 14 dB. After 1 - 2 days of freezing the grease ice starts to form pancake ice with characteristic edges which causes high radar return, typically above - 7.0 dB. As the pancake ice grows thicker during the winter it forms 1 - 2 m thick firstyear ice. The ice in this zone is constantly exposed to surface waves and is therefore characterized by a rough surface. Grease ice and calm water (wind speed below 3 m/s) can have overlapping backscatter values which makes the interpretation of the SAR images ambiguous, however no wind speeds below 3 m/s were observed in the experiment. Open water in the SAR images had higher backscatter than any of the observed ice types, from - 4.5 to - 3.0 dB. The backscatter values for the most important ice types in the Barents Sea is summarized in Fig. 4.

Summer conditions

The classification into three zones suggested for winter conditions would not be valid in the summer. Zone C with ice formation would be absent. Zone A and B would be detectable, but the discrimination between different ice types becomes less significant. Due to wet snow and melt water on top of the ice the SAR backscatter values from multiyear floes is reduced compared to the winter situation and becomes similar to the signature for firstyear ice. It is therefore difficult to separate the two ice types based solely on backscatter levels (Shuchman and Onstott, 1990; Frette et al., 1992). Thin ice types such as grease ice, pancake ice and young ice are usually not found in the summer.

4. ICE EDGE DEFINITION

Previous investigations of the marginal ice zone show that the ice edge can have a variable configuration depending on the wind, wave and current conditions (Johannessen et al., 1983, Johannessen et al., 1987, Sandven and Johannessen 1993). It can be compact or diffuse, straight or meandering with tongues of ice extending out in open water. The SAR instrument has been the most important tool to map the ice edge and its variability. The ice edge definition in the SAR images depends on the differences between ice and open water signature. In contrast to the ice signatures, the open water signature is heavily dependent on wind conditions and viewing geometry (Moore and Fung, 1979). As dicussed above open water had higher backscatter than the ice types observed during the experiment. Therefore the ice edge could be defined in all the SAR images, but the contrast in signature between ice and open water varied.

On March 2 the ice edge was straight and sharp due to on-ice wind of 6 - 8 m/s during the preceding days and the SAR profile showed a well-defined edge. The backscatter profile across the ice edge increased from about -13 dB within the firstyear ice to about -4.5 dB in open

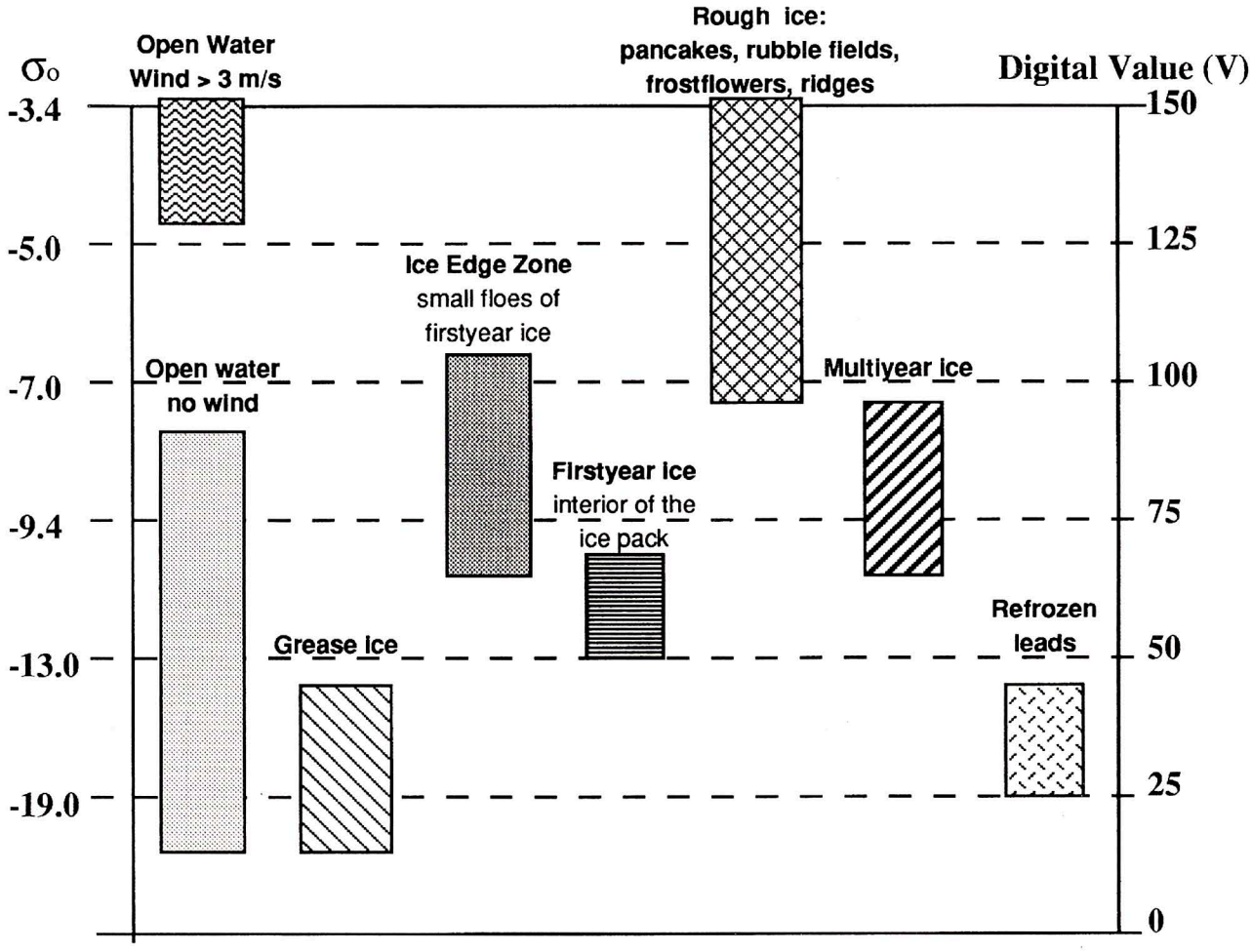

Relation between σ_o and V:

$$\sigma_o = 20 \log V - 46.9$$

assuming V = 14 corresponds to a noise floor of - 24 dB

Fig. 4 - Summary of backscatter values for different ice types in the Barents Sea during winter conditions

water (Fig. 5 a). In most cases, however, the ice edge is less compact with a more diffuse transition from areas of lower to higher ice concentration. Six days later, on March 6, the ice edge was meandering and more diffuse due to variable wind conditions (Fig. 3). The SAR profile showed a less pronounced edge, but with a gradient of about 3 dB it was still well-defined (Fig. 5 b). The profile also showed some bands of open water just inside of the ice edge. In the south end of the profile there is a strong gradient of 14 dB from open water to grease ice. During summer conditions with diffuse ice edge and wet ice we have seen examples of SAR images where it is very difficult to identify the ice edge (Kloster et al., 1992 a).

5. ICE CONCENTRATION

An ice concentration algorithm, developed at NERSC for airborne SAR imagery (Sandven et al., 1991), has been modified for use with ERS-1 SAR data. Ice concentration is defined as the percentage of a unit area covered by sea ice. The parameter can be derived from various remote sensing sensors capable of separating ice from water, such as SAR. The first step in the algorithm is to distinguish the major ice types from open water based on the backscatter values shown in Fig. 4. Most of the ice signatures such as firstyear and multiyear ice are in the range from a lower threshold value of - 13 to an upper value of about - 6 dB. The algorithm applies these two threshold values to sepa-

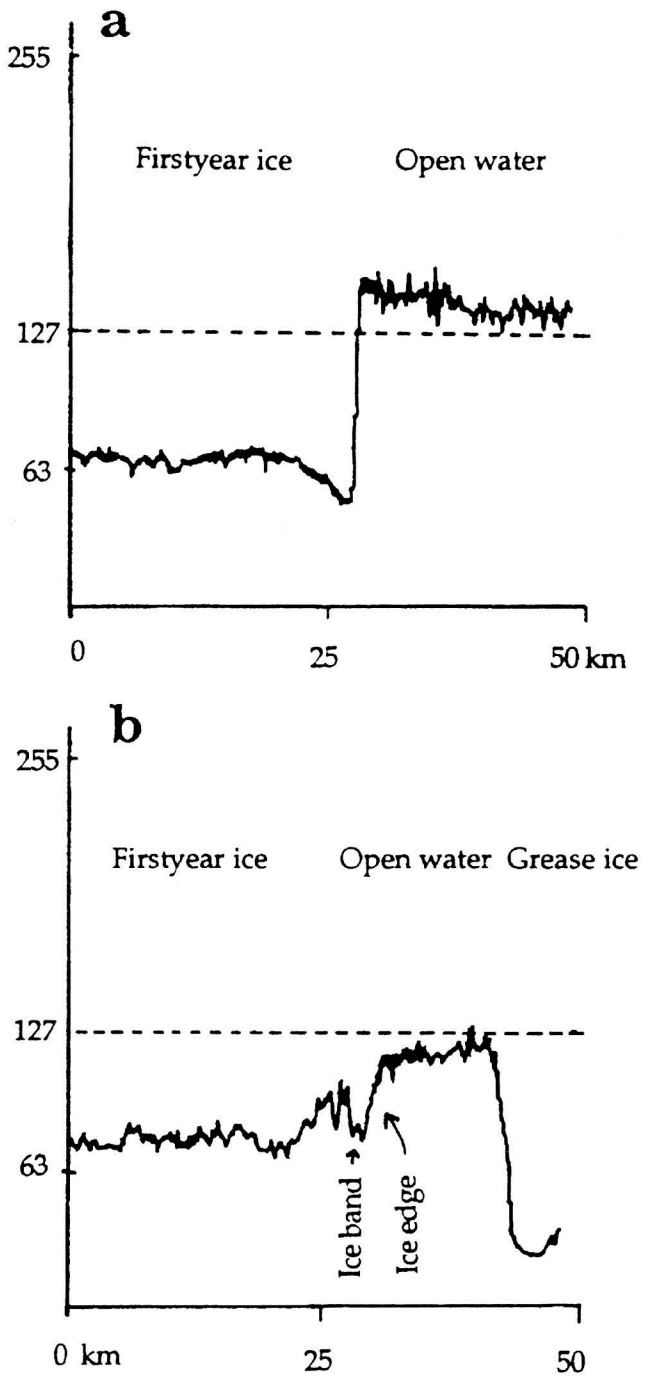

Fig. 5 - SAR backscatter profiles across the ice edge on March 2 (a) and March 8 (b)

rate pixels with thick ice. The highest signatures, representing open water and most of the pancake ice, ridges and rubble fields, are classified as non-ice pixels. The grease ice and calm water, which is defined by the lower threshold level, is also is also classified as non-ice. The pixels between -13 and -6 dB, are defined as ice pixels. The ice concentration calculations from this algorithm have been compared with estimates from aerial photographs and SSM/I data.

The algorithm gives reasonable results in most of the images analyzed in Zone A and B. In zone B, where the concentration was typically 95 %, the algorithm provided estimates of 100 %. This is due to the fact that the SAR imagery was unable to resolve the small open leads constituting about 5 % of the ice area. In zone C the results were in some cases inaccurate because the SAR signatures of new ice changed rapidly and overlapped with the open water signature. To improve the algorithm in the ice edge region a better ice type classification is required for this region.

5. ICE KINEMATICS

An ice kinematics algorithm (Sandven et al.,1991, Kloster et al., 1992 b) was applied to the SAR images in the D17 swath obtained on March 2, 5, 8 and 11. The principle of the algorithm is to recognize features, using a correlation between subimages in the two input images which must be obtained in the same area at different times. The algorithm applies two-dimensional binary search in pairs of sub-images to reduce the total number of correlations to be setimated. The results of algorithm were reasonable when applied in the interior of the ice pack (zone A) where the larger floes and leads could be identified. The calculated ice vectors were tested against manually derived vectors and with a drifting buoy. In the three-day period from March 8 to 11 a drifting buoy with Argos system provided positions of the buoys every three hour. These positions were lowpass-filtered to remove the tidal motion from the ice drift. From the drift data a three-day mean displacement vector was calculated and compared with the vectors from the SAR algorithm, showing good agreement. In zone B and C the algorithm could not produce any velocity vectors because of the uniform signature in the images.

6. CONCLUSIONS FROM SIZEX 92

In the SIZEX 92 experiment ERS-1 SAR scenes of all the major ice types in the Barents Sea were analyzed for winter conditions. These include:

a) 3 - 4 m thick multiyear ice floes which originate from the Arctic Ocean north of Svalbard.
b) refrozen leads with smooth thin ice.
c) consolidated firstyear ice 2 - 3 m thick which is formed between multiyear floes in the interior of the ice pack during the present winter season.

d) rough ice in leads, ridges and rubble fields.
e) first year ice 2 - 3 m thick in a 20 - 30 km wide zone inside the ice edge broken up in typically 10 - 50 m large floes due to wave action.
f) new ice formed outside the ice edge (grease ice and pancake ice).

The most difficult factor which influences the SAR ice classification and ice concentration algorithms is the variable backscatter from open water due to the wind speed. Open water can have similar signature to some of the ice types, in particular pancake ice and first year ice with rough surface. In order to improve the algorithm for ice type determination and thus also for the ice edge detection and ice concentration estimation, it is necessary to know the SAR signature for the ice types and their surface characteristics more quantitatively. SAR data from summer conditions, obtained in August 91, have been a very useful supplement to the winter data and demonstrated that multiyear and firstyear ice can have similar signatures during summer conditions.

The main result of the SIZEX program is the improvement in the knowledge of different ice signatures in ERS-1 SAR data. Although there are many unresolved questions concerning SAR signatures of sea ice, SAR data are expected to play an important role in future ice monitoring systems.

ACKNOWLEDGEMENT

The SIZEX 92 project has been supported by the European Space Agency, the Norwegian Space Agency, Operatørkomite Nord (OKN), Office of Naval Research, and the University of Bergen.

REFERENCES

Caneva N., ERS-1 SAR calibration, Frascati, October 1, 1992.

Frette Ø. & al., SIZEX 91. ERS-1 SAR and in situ observations of sea ice during the Lance cruise in August 1991. NERSC Special Report no. 13, June 1992.

Johannessen O.M., Johannessen J.A., Morison J., Farrelly B.A. & Svendsen E.A., 1983, Oceanographic conditions in the marginal ice zone north of Svalbard in early fall 1979 with emphasis on mesoscale processes. J. Geophys. Res., Vol. 88, pp. 2755-2769.

Johannessen O.M. & al., SIZEX. Seasonal Ice Zone Experiment. ERS-1 pre- and postlaunch program in the Barents Sea, Fram Strait and Greenland Sea. NERSC Technical report No. 61, Nov. 1986.

Johannessen J.A., Johannessen O.M., Shuchman R., Manley T., Campbell W.J., Josberger E.G., Sandven S., Gascard J.C., Olaussen T., Davidson K. & van Leer J., 1987, Mesoscale eddies in the Fram Strait marginal ice zone during the 1983 and 1984 Marginal Ice Zone Experiment. J. Geophys. Res., Vol. 92, pp. 6754-6772.

Johannessen O.M., Sandven S., Campbell W.J. & R. Shuchman. Ice studies in the Barents Sea by ERS-1 SAR during SIZEX 92. Paper presented at the First ERS-1 Symposium, Cannes, 4 -6 November 1992.

Johannessen O.M. & al., 1992 a. ERS-1 SAR ice routing of L`Astrolabe through the Northeast Passage. Proceedings of the Central Symposium of the 'International Space Year' Conference, Munich, Germany, 30 March – 4 April 1992. ESA SP-341, pp. 997-1002 July 1992.

Johannessen O.M. & al., 1992 b. Microwave Study Programs in the Seasonal Ice Zone of the Greenland and Barents Seas. Chapter 13 in Microwave Remote Sensing of Sea Ice (edited by F. Carsey).

Kloster K., Johannessen O.M., Sandven S. & Frette Ø., The Northern Sea Route. Analysis of ERS-1 SAR data from August 1991. NERSC Special Report No. 2. March 1992 a.

Kloster K., Flesche H. & Johannessen O.M., 1992 b, Ice motion from airborne SAR and satellite imagery. Adv. Space Res. Vol. 12, No. 7, pp 149-153.

Moore R.K. & Fung A.K., Radar determination of winds at sea. Proc. IEEE, 67, 1504-1521, 179.

Sandven S., Kloster K. & Johannessen O.M., SAR ice algorithms for ice edge, ice concentration and ice kinematics. NERSC Technical Report No. 38, February 1991.

Sandven S. & al., 1992. SIZEX 92. ERS-1 SAR ice validation experiment in the Barents Sea. NERSC Technical Report No. 65, November 1992.

Sandven S. & Johannessen O.M., 1993, The use of microwave remote sensing for sea ice studies in the Barents Sea. ISPRS Journal of Photogrammetry and Remote Sensing, 48(1), pp. 2-18.

Shuchman R.A. & Onstott R.G., 1990, Remote sensing of Polar Oceans. In Polar Oceanography, Part A: Physical Science (Edited by W.O. Smith jr.) pp. 123-169.